SparseRNAFolD: Sparse RNA pseudoknot-free Folding including Dangles

Mateo Gray, Sebastian Will, Hosna Jabbari

SparseRNAFolD: Sparse RNA pseudoknot-free Folding including Dangles

Mateo Gray
Department of Biomedical Engineering, University of Alberta, Canada

Sebastian Will
CNRS/LIX (UMR 7161), Institut Polytechnique de Paris, France

Hosna Jabbari
Department of Biomedical Engineering, University of Alberta, Canada

Abstract

Motivation:
Computational RNA secondary structure prediction by free energy minimization is indispensable for analyzing structural RNAs and their interactions. These methods find the structure with the minimum free energy (MFE) among exponentially many possible structures and have a restrictive time and space complexity ($O(n^3)$ time and $O(n^2)$ space for pseudoknot-free structures) for longer RNA sequences. Furthermore, accurate free energy calculations, including dangles contributions can be difficult and costly to implement, particularly when optimizing for time and space requirements.
Results:
Here we introduce a fast and efficient sparsified MFE pseudoknot-free structure prediction algorithm, SparseRNAFolD, that utilizes an accurate energy model that accounts for dangle contributions. While the sparsification technique was previously employed to improve the time and space complexity of a pseudoknot-free structure prediction method with a realistic energy model, SparseMFEFold, it was not extended to include dangle contributions due to the complexity of computation. This may come at the cost of prediction accuracy. In this work, we compare three different sparsified implementations for dangles contributions and provide pros and cons of each method. As well, we compare our algorithm to LinearFold, a linear time and space algorithm, where we find that in practice, SparseRNAFolD has lower memory consumption across all lengths of sequence and a faster time for lengths up to 1000 bases.
Conclusion:
Our SparseRNAFolD algorithm is an MFE-based algorithm that guarantees optimality of result and employs the most general energy model, including dangle contributions. We provide a basis for applying dangles to sparsified recursion in a pseudoknot-free model that has the ability to be extended to pseudoknots.
Availability:
SparseRNAFolD's algorithm and detailed results are available at `https://github.com/mateog4712/SparseRNAFolD`.

2012 ACM Subject Classification Applied computing → Molecular structural biology

Keywords and phrases RNA, MFE, Secondary Structure Prediction, Dangle, Sparsification, Space Complexity, Time Complexity

Digital Object Identifier 10.4230/LIPIcs.WABI.2023.20

Related Version *Previous Version*: `https://www.biorxiv.org/content/10.1101/2023.06.05.543808v1`

1 Introduction

Non-coding RNAs play crucial roles in the cell, such as in transcription [3], translation [3, 16], splicing [23, 32], catalysis [3, 36] and regulating gene expression [3, 12, 18, 23]. Since RNA's function heavily relies on its molecular structure, facilitated by hydrogen bonding both within and between molecules, predicting and comprehending the structure of RNA is a dynamic

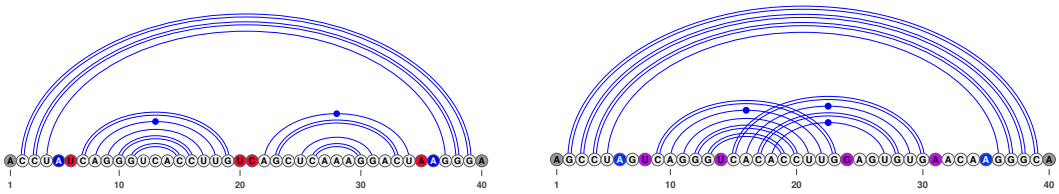

(a) Pseudoknot-free **(b)** Pseudoknotted

Figure 1 An RNA structure is shown with dangles highlighted. **(a)** In red, we have the dangles on the bands in the multi-loop. In blue, we have the dangle on the closing bases of the multi-loop. In gray, we have dangles on the outer end of the RNA. **(b)** We include purple to show dangles occurring in a pseudoknot. Dangles in pseudoknots can be handled differently depending on the program.

area of research. It is reasonable to assume (without further knowledge) that RNA forms the structure with the lowest free energy [19, 24]. This is the motivation for algorithms that aim to predict the RNA minimum free energy (MFE) structure from the pool of exponentially many structures it can form. Such methods employ a set of energy parameters for various loop types, called an energy model; to find the free energy of a structure, they add up the energy of its loops. While prediction accuracy of these methods depends on the quality of their energy models, these methods are applicable to novel RNAs with unknown families or functions and for the prediction of the structure of interacting molecules. The large time and space complexity of MFE-based methods ($O(n^3)$ time and $O(n^2)$ space where n is the length of the RNA), however, restricted their applications to small RNAs. The sparsification technique was recently utilized in existing MFE-based algorithms to reduce their time and/or space complexity [34, 29, 22, 2, 4, 35, 15, 14] by removing redundant cases in the complexity-limiting steps of the dynamic programming algorithms. While the majority of these methods focused on simple energy models, some expanded sparsification techniques to more realistic energy models [35, 15, 14]. To the best of our knowledge, no existing method has yet incorporated dangles energy contributions into a sparsified prediction algorithm. Dangle energies refer to the free energy contributions of unpaired nucleotides that occur at the end of a stem-loop structure.

We show in Figure 1 the location of dangles on a pseudoknot-free structure (see Figure 1a) and a pseudoknotted structure (see Figure 1b). The complexity of dangles in a pseudoknot further increases as dangles have to be tracked for both bands within the pseudoknot.

Neglecting dangle energies in the prediction of RNA structure stability can lead to inaccuracies. For instance, a stem-loop structure that includes an unpaired nucleotide at the end may appear less stable than its actual stability if the dangle energy contribution is ignored. Conversely, a stem-loop structure with an unpaired nucleotide that interacts positively with another one may appear more stable than its actual stability if the dangle energy contribution is not taken into account.

Dangles, in some form, are implemented in the majority of MFE pseudoknot-free secondary structure prediction algorithms [9, 8]. RNAFold [9, 11, 21, 6, 17, 41, 7] is an $O(n^3)$ time and $O(n^2)$ space algorithm which implements the dangle 0 (“no dangle”), dangle 2 (“always dangle”), and dangle 1 (“exclusive dangle”) model (defined in Section 2.1). It also utilizes a dangle model that implements coaxial stacking – a type of stacking that gives a bonus to stacks in the vicinity of each other. LinearFold [8], a sparsified $O(n)$ space heuristic algorithm has implemented the “no dangle” and “always dangle” model but has not implemented an “exclusive dangle” model. Fold from the RNAstructure library [27] is an $O(n^3)$ time and

$O(n^2)$ space algorithm which implements an "exclusive dangle" model with coaxial stacking. MFold [40, 33, 39] is an $O(n^3)$ time and $O(n^2)$ space algorithm which has implemented an "exclusive dangle" model with coaxial stacking.

Handling dangles in pseudoknot prediction algorithms are less developed. Pknots [28], an $O(n^6)$ time and $O(n^4)$ space pseudoknot prediction algorithm has implemented an "exclusive dangle" model that also includes coaxial stacking. Within Pknots, a set of parameters is defined for non-pseudoknot and pseudoknot dangles. The pseudoknot parameters are estimated and rely on an estimated weighting parameter. Hotknots [26], a heuristic algorithm, uses the DP09 parameters, which include pseudoknotted parameters from Dirks and Pierce [5] and tuned by Andronescu et al. [26]; however, the energies for the pseudoknotted dangles are the same as those for pseudoknot-free dangles, and there is no weighting parameter.

Contributions. In [35], we already discussed the sparsification of RNA secondary structure prediction by minimizing the energy in the Turner energy model. However, in this former work, we did not yet consider the energy contributions due to the interactions of base pairs at helix ends with dangling bases (i.e., 'dangling ends'). Here, we identify the correct handling of dangling end energies in the context of sparsification as a non-trivial problem, characterize the issues, and present solutions.

For this purpose, we first state precisely how dangle energies are handled by energy minimization algorithms; to the best of our knowledge, this is elaborated here for the first time. Consequently, we devise novel MFE prediction algorithms that include dangling energy contributions *and* use sparsification techniques to significantly improve the time and space complexity of MFE prediction.

Like the algorithm in [35], our efficient SparseRNAFolD algorithm keeps the additional information to a minimum using garbage collection. In total, we study three different possible implementations and compare their properties, which make them suitable for different application scenarios. Finally, while we study the case of non-crossing structure prediction, we discuss extensions to the more complex cases of pseudoknot and RNA–RNA interaction prediction (such extensions being the main motivation for this work in the first place).

2 Preliminaries: sparsification without dangling ends

We restate the preliminaries and main results from our former work on sparsification of free energy minimization without dangling ends [35].

We represent an ***RNA sequence*** of length n as a sequence $S = S_1, \ldots, S_n$ over the alphabet $\{A, C, G, U\}$; $S_{i,j}$ denotes the ***subsequence*** $S_i, \ldots, S_j$. A ***base pair*** of S is an ordered pair $i.j$ with $1 \leq i < j \leq n$, such that ith and jth bases of S are complementary (i.e. $\{S_i, S_j\}$ is one of $\{A, U\}, \{C, G\}$, or $\{G, U\}$). A ***secondary structure*** R for S is a set of base pairs with at most one pair per base (i.e. for all $i.j$, $i'.j' \in R$: $\{i, j\} \cap \{i', j'\} = \emptyset$). Base pairs of secondary structure R partition the unpaired bases of sequence S into ***loops*** [25] (i.e., hairpin loop, interior loop and multiloop). Hairpin loops have a minimum length of m; consequently, $j - i > m$ for all base pairs $i.j$ of R. Two base pairs $i.j$ and $i'.j'$ cross each other iff $i < i' < j < j'$ or $i' < i < j' < j$. A secondary structure R is ***pseudoknot-free*** if it does not contain ***crossing base pairs***.

The unsparsified, original algorithm for energy minimization over pseudoknot-free secondary structures was stated by Zuker and Stiegler [42]. It is a dynamic programming algorithm that, given an RNA sequence S of length n, recursively calculates the minimum free energies (MFEs) for subsequences $S_{i,j}$ as $W(i, j)$ (stored in a dynamic programming matrix). Finally, $W(1, n)$ is the optimal free energy. We state this algorithm in a sparsification-friendly form

following [35]. As usual, the algorithm is described by a set of recursion equations (for a minimum hairpin loop size of m and a maximum interior loop size of M). For $1 \leq i < j \leq n$, $i < j - m$:

$$W(i,j) = \min\{\, W^p(i,j), V(i,j) \,\} \tag{1}$$

$$W^p(i,j) = \min\{\, W(i,j-1), \min_{i<k<j} W(i,k-1) + W(k,j) \,\} \tag{2}$$

$$V(i,j) = \min\{\mathcal{H}(i,j); \min_{\substack{i<p<q<j \\ p-i+j-q-2\leq M}} \mathcal{I}(i,j;p,q) + V(p,q); WM^2(i+1,j-1) + a\} \tag{3}$$

$$WM(i,j) = \min\{\, WM^p(i,j), V(i,j) + b \,\} \tag{4}$$

$$WM^p(i,j) = \min\{\, WM(i+1,j) + c, WM(i,j-1) + c, WM^2(i,j) \,\} \tag{5}$$

$$WM^2(i,j) = \min_{i<k<j} WM(i,k-1) + WM(k,j). \tag{6}$$

Here, a, b, c are multi-loop initialization penalty, branch penalty, and unpaired penalty in a multi-loop, respectively. $\mathcal{I}(i,j;p,q)$ refers to an interior loop between base pairs i.j and p.q. The initialization cases are $W(i,i) = 0$; $V(i,j) = WM(i,j) = \infty$ for all $j - i \leq m$ and $WM^2 = \infty$ for all $j - i \leq 2m + 3$.

In these recursions, all function values (like $W(i,j)$ or $W^p(i,j)$) denote minimum free energies over certain classes of structures of subsequences $S_{i,j}$. The classical Zuker/Stiegler matrices W, V and WM are defined as: W yields the MFEs over general structures; V, over closed structures, which contain the base pair $i.j$; WM, over structures that are part of a multi-loop and contain at least one base pair.

Since sparsification is based on the idea that certain optimal structures can be decomposed into two optimal parts, while others (namely closed structures) are non-decomposable, we single out the partitioning cases and introduce additional function symbols W^p, WM^p, and WM^2.

Sparsification without dangling ends. This allows us to cleanly explain the *key idea of sparsification* and consequently formalize it: to minimize over the energies of general structures in $W(i,j)$—note that there is another minimization inside of multi-loops that is handled analogously—the algorithm considers all closed structures $V(i,j)$ and all others $W^p(i,j)$. Optimal structures in the latter class can be decomposed into two optimal structures of some prefix $S_{i,k-1}$ and suffix $S_{k,j}$ of the subsequence. Classically, the minimum is therefore obtained by minimizing over all ways to split the subsequence. Sparsification saves time and space since it is sufficient to consider only the splits where the optimum of the suffix $S_{k,j}$ is not further decomposable (formally, where $W(k,j) < W^p(k,j)$). Briefly (for more detail, see [35] or [34]), this is sufficient since otherwise there is a k' to optimally split the suffix further into $S_{k,k'-1}$ and $S_{k',j}$. The split of $S_{i,j}$ at k cannot be better than the split at k' and therefore does not have to be considered in the minimization; thus, it can be restricted to a set of *candidates*. This is argued by the ***triangle inequality for*** W (which directly follows from the definition of W as minimum):

$$W(i,j) \leq W(i,k-1) + W(k,j) \qquad \text{for all } 1 \leq i < k \leq j \leq n.$$

Consequently, sparsification improves the computation of W^p, WM^p and WM^2. The

corresponding sparsified version are

$$\widehat{W}^{\mathrm{p}}(i,j) = \min\{\, W(i,j-1); \min_{[k,j] \text{ is candidate}, k>i} W(i,k-1) + V(k,j) \,\}$$

$$\widehat{WM}^{\mathrm{p}}(i,j) = \min\{\, WM(i,j-1) + c; \min_{[k,j] \text{ is candidate}, k>i} c \cdot (k-i) + V(k,j) \,; WM^2(i,j)\}$$

$$\widehat{WM}^{2}(i,j) = \min\{\, WM^2(i,j-1) + c; \min_{[k,j] \text{ is candidate}, k>i} WM(i,k-1) + V(k,j) \,\}$$

where candidates $[k,j]$ correspond to the not optimally decomposable subsequences $S_{k,j}$ (in either situation: general structures or structures inside of multi-loops), i.e. $[i,j]$ is a ***candidate*** iff $V(i,j) < \widehat{W}^{\mathrm{p}}(i,j)$ or $V(i,j) + b < \widehat{WM}^{\mathrm{p}}(i,j)$.

Time and space complexity of sparsified energy minimization. Will and Jabbari showed that following the above algorithm, $W(1,n)$ can be calculated in $O(n^2 + nZ)$ time, where Z is the total number of *candidates*. While the MFE structure in the Zuker and Stiegler algorithm can be trivially reconstructed following a traceback procedure, this is not the case if sparsification is used for improving time *and* space as in the SparseMFEFold algorithm (and our novel algorithms). To improve the space complexity, sparsification avoids storing all entries of the energy matrix. The idea is to store the candidates and as few additional matrix entries as possible. A specific challenge is posed by the decomposition of interior loops (the single most significant major complication over base pair maximization, see [2]). For this reason, Will and Jabbari introduced *trace arrows* for cases, where the trace cannot be recomputed efficiently during the traceback procedure; they discussed several space optimization techniques, such as avoiding trace arrows by rewriting the MFE recursions, and removing trace arrows as soon as they become obsolete. Due to such techniques, SparseMFEFold requires only linear space in addition to the space for candidates and trace arrows; its space complexity is best described as $O(n + T + Z)$, where T is the maximum number of trace arrows.

2.1 Dangles

Recall that sparsification was discussed before (e.g., in SparseMFEFold) only for the simplest and least accurate variant of the Turner model, namely the one without dangling end contributions. Before we improve this situation, let's look in more detail at dangling ends and different common ways to handle them. Specifically, we discuss different *dangle models* "no dangle" (model 0), "exclusive dangle" (model 1), and "always dangle" (model 2) as implemented by RNAFold of the Vienna RNA package (and available via respective command line options `-d0`, `-d1`, and `-d2`).

Dangling end contributions occur only at the ends of stems (either in multiloops or externally) due to stacking interaction between the closing base pair of the stem and one or both immediately adjacent unpaired bases. In contrast, dangling end terms are not considered within (interior loops of) stems by the energy model.

We present modified DP recursions in order to reflect precisely where and how dangling ends are taken into account. Therefore, in preparation, let's replace V in the Equations (1) and (4) of the free energy minimization recursions of Section 2 by a new function V^{d}. The dangle models differ in the exact definition of V^{d}.

$$W(i,j) = \min\{\, W^{p}(i,j), V^{\mathrm{d}}(i,j) \,\} \tag{1'}$$

$$WM(i,j) = \min\{\, WM^{p}(i,j), V^{\mathrm{d}}(i,j) + b \,\} \tag{4'}$$

Note that in the energy model, dangling ends can also occur at the inner ends of helices that close a multi-loop. These dangles can be handled directly in the recurrence of $V(i,j)$; specifically, in the subcase where $i.j$ closes a multi-loop.

No dangles. In the simplest model "no dangle", dangling ends are ignored. We achieve this by defining

$$V^{\mathrm{d}}(i,j) := V(i,j) \qquad \text{(no dangle)}$$

While easy to implement, it is clearly wrong to ignore dangling end contributions, and this has a significant negative effect on the prediction accuracy compared to the other dangle models [30, 38, 37].

Always dangle. A second relatively simple way is to apply a 53' dangle energy at both ends of a stem (both 5' and 3' ends), assuming that stem ends always dangle with their adjacent bases. As a strong simplification, in this model, one disregards whether the bases are paired and/or dangle with a different stem (either case would actually make them unavailable for dangling).

This dangle model allows the dangling ends to have a thermodynamic influence while keeping the model easy to implement as neither the conflicting adjacent nucleotides nor the energies of single dangle have to be tracked; it only requires knowledge of the bases on the 3' and 5' sides of a base pair. Formally, we implement V^{d} as

$$V^{\mathrm{d}}(i,j) := V(i,j) + \mathrm{dangle}_{53}(i,j) \qquad \text{(always dangle)}$$

Moreover, we add the appropriate dangle contribution when closing a multi-loop in Eq. (3) in the last case of the V-recurrence of Eq. (3). The term $WM^2(i+1,j-1)+a$ is rewritten to

$$WM^2(i+1,j-1) + a + \mathrm{dangle}_{53}(i+1,j-1) \qquad \text{(always dangle, ML closing)}$$

Exclusive dangling. The most complex but general secondary structure dangle model, "exclusive dangle" considers both single and double unpaired nucleotides adjacent to a stem. Furthermore, the model does not allow shared dangling ends i.e. no base can be used simultaneously in two dangles (in other words, adjacent unpaired bases dangle *exclusively* with a single stem end). As the restriction requires tracking of unpaired bases, $V(i,j)$ places the possible unpaired bases at i and j and looks at the adjacent V energies. As this requires knowledge of energies adjacent to the current bases being looked at, this inherently causes difficulty in sparsification.

$$V^{\mathrm{d}}(i,j) := \min \begin{cases} V(i,j) \\ V(i+1,j) + \mathrm{dangle}_5(i) \\ V(i,j-1) + \mathrm{dangle}_3(j) \\ V(i+1,j-1) + \mathrm{dangle}_{53}(i,j) \end{cases} \qquad \text{(exclusive dangle)}$$

Moreover, we consider dangles at the closing of a multi-loop. In this model, the case $WM^2(i+1,j-1)+a$ in the minimization of Eq. (3) is replaced by (the minimum of) four different cases:

$$\min \begin{cases} WM^2(i+1,j-1) + a \\ WM^2(i+2,j-1) + a + \mathrm{dangle}_3(i) \\ WM^2(i+1,j-2) + a + \mathrm{dangle}_5(j) \\ WM^2(i+2,j-2) + a + \mathrm{dangle}_{53}(i,j) \end{cases} \qquad \text{(exclusive dangle, ML closing)}$$

2.2 Space-efficient sparsification with exclusive dangles is non-trivial

We approach our main motivation for this work, which is to study and solve the issues of sparsification in the exclusive dangle model (dangle model 1). Let's thus start by applying the idea of sparsification (Section 2) straightforwardly to the Recursion (2) (where W and V^{d} are defined for exclusive dangles).
We quickly come up with the equation:

$$\widehat{W}^{\mathrm{p}}(i,j) = \min\{\, W(i,j-1); \min_{[k,j] \text{ is ed-candidate}, k>i} W(i,k-1) + V^{\mathrm{d}}(k,j)\,\},$$

but we would still have to define *ed-candidate* (exclusive dangle candidate) to make this work. We could define: [i,j] is an ***ed-candidate*** iff $V^{\mathrm{d}}(i,j) < \widehat{W}^{\mathrm{p}}(i,j)$, where the correctness of sparsification holds to a sparsification-typical triangle inequality argument (Section 2).

Expanding V^{d} shows that this is not the only possible path to sparsifying the recursion. We could consider

$$\widehat{W}^{\mathrm{p}}(i,j) = \min \begin{cases} W(i,j-1) \\ \min_{[k,j] \text{ is ed0-candidate}, k>i} W(i,k-1) + V(i,j) \\ \min_{[k,j] \text{ is ed5-candidate}, k>i} W(i,k-1) + V(i+1,j) + \mathrm{dangle}_5(i) \\ \min_{[k,j] \text{ is ed3-candidate}, k>i} W(i,k-1) + V(i,j-1) + \mathrm{dangle}_3(j) \\ \min_{[k,j] \text{ is ed53-candidate}, k>i} W(i,k-1) + V(i+1,j-1) + \mathrm{dangle}_{53}(i,j) \end{cases}$$

with different sets of candidates for all four cases. However, storing all these candidate sets (recall that there is even a second recursion that needs to be sparsified) is easily prone to compromising any space benefits due to sparsification in practice.

The transfer of the techniques from [35] brings even more problems, since due to such definitions, candidates [i,j] do not necessarily correspond to subsequences that have closed optimal structures. Will and Jabbari strongly exploited this fact for their strong space savings.

Even considering our definition of an ed-candidate, we still run into the challenge of to tracing back to the corresponding base pair. With just the dangle energy, this poses issues as an ed-candidate can be one of four cases.

▶ **Lemma 1.** *In the exclusive dangle model, storing only the energy of each ed-candidate is not sufficient to correctly trace back from the candidate.*

Proof. Concretely, for the loop-based Turner 2004 energy model [20]) with exclusive dangles, consider the following RNA sequence S of length 12 with its MFE structure:

```
UGGGAAAACCCC
.(((....))).
```

In the calculation of $W(1,12)$, the recurrences unfold to $W(1,12) = W(1,1) + V^{\mathrm{d}}(2,12) = W(1,1) + V(2,11) + \mathrm{dangle}_3(12) = \cdots = -2.9$ kcal/mol, i.e. it is optimal to assume dangling of base pair $(2,11)$ to the right.

In a non time- and space-sparsified algorithm, recomputing V^{d} from V adjacent energies would be trivial. However, due to space sparsification, the values of V are generally unavailable in the trace-back phase. In the constructed example, recomputation would require us to know $V(2,12)$, $V(2,11)$, $V(3,12)$, and $V(3,11)$. Thus, under the assumption of the lemma, the optimal dangling cannot be efficiently recomputed for a candidate like [2,12]. ◀

In our preceding work SparseMFEFold [35], trace arrows were introduced to trace back to non-candidate values necessary to the structure within the interior loop case: $V^{\text{il-cand}}(i,j)$. Trace arrows that point to candidates are not stored as they can be avoided by minimizing over candidates as seen in Equation 7.

$$V^{\text{il-cand}}(i,j) = \min_{\substack{i<p<q<j \\ p-i+j-q-2\leq M \\ [p,q] \text{ is candidate}}} \mathcal{I}(i,j;p,q) + V(p,q). \tag{7}$$

Consequently, finding the inner base pair of a loop through a candidate relies on the energy saved being $V(p,q)$. However, as shown in Eq. (exclusive dangle, ML closing), the dangle energy could be $V(p,q)$, $V(p+1,q)$, $V(p,q-1)$, or $V(p+1,q-1)$. Replacing the stored energy within a candidate with V^{d} may conflict with the interior loop calculation. Recomputation of the V values required for V_d would negate the sparsification benefit. In summary, there is no easy or direct way to save the V energy required for the interior loop as well as the V^{d} energy required for a multi-loop or external loop within the current candidate structure.

▶ **Lemma 2.** *The minimization over inner base pairs in the recursion of V cannot be restricted to candidates in the same way as in SparseMFEFold.*

Proof. Again consider the loop-based Turner 2004 energy model. There is a sequence S and $1 \leq i < j \leq n$, such that $V^{\text{d}}(p,q) < V(p,q)$, but there is no way to trace back to p and q from i and j, namely, consider the RNA sequence S of length 19 with its MFE structure:

```
GGGAGGGAAAACCCCACCC
(((.(((.....))).)))
```

The optimal recursion case of $V(3,17)$ forms the interior loop closed by 3.17 with inner base pair 5.15, because $V(5,15) = -2.4$ kcal/mol and V(3,17) $= \mathcal{I}(3,17;5,15) + V(5,15) = -1.5$ kcal/mol.

The space optimization of SparseMFEFold removes trace arrows to candidates since the trace-back to candidates can be reconstructed based on candidate energies (compare Eq. (7).

In the way of SparseMFEFold, we would not store a trace arrow pointing to 5.15 from $[3,17]$, since $[5,15]$ is a candidate. However, without a trace arrow, we would not reconstruct the correct trace. This happens, since the optimal structure in the subsequence 5..15 `GGGAAAACCCC` would be `(((....)))`. due to the 3' dangle ($V^{\text{d}}(5,15) = -2.9$ kcal/mol). Consequently, tracing back the optimal path from $V^{\text{d}}(5,15)$ wrongly introduces a base pair at 5.14. ◀

3 SparseRNAFolD

SparseRNAFolD combines the power of sparsification and a general energy model including dangle energies to achieve a fast and highly accurate RNA pseudoknot-free secondary structure prediction. To this end, we started with the sparsified dynamic programming recurrences of SparseMFEFold (which implements the "no dangles" model), rewriting and revising them to accommodate various dangle energies.

3.1 "always dangle" model

Recall that "always dangle" model considers both the 5' and 3' ends of a branch of a multi-loop or external loop for dangle contributions. The addition of this model is trivial, with no

change necessary to the recurrences of the SparseMFEFold. Note that, as mentioned earlier, this model ignores overlapping cases and may overcount the contributions of dangles.

3.2 "exclusive dangle" model

As mentioned in Section 2.2, accounting for the "exclusive dangle" model is non-trivial when dealing with candidates, as ed-candidates do not hold enough information to identify the direction of dangles. To alleviate this problem, we provide three different strategies, as described below. Each strategy has its pros and cons and should be selected based on the application.

In order to handle the changes for exclusive dangles, we extend the candidate data structure. A candidate base pair, $[i, j]$ as implemented in SparseMFEFold, holds i, the start position, and the energy $V(i, j)$ as a tuple $(i, V(i, j))$ and is stored at the jth index of the candidate list. Our extensions to candidate structures involves including the energy values for W and WM in the candidate tuples as $(i, V(i, j), W(i, j), WM(i, j))$. The modification reflects the need to store more information about the dangles positions and directions.

Strategy 1: Trace Arrow implementation

As the first strategy to trace an ed-candidate to its position, we used modified trace arrows. We refer to this strategy as **SparseRNAFolD-Trace**.

Recall that in SparseMFEFold, a trace arrow structures were introduced to identify energy matrix entries that are necessary for calculating the energy of internal loops but are not kept as candidates. Here, we define ***ed-trace-arrows*** to hold information about dangle positions to aid with the traceback procedure from ed-candidates. In particular, in the sparse fold reconstruction procedure of SparseRNAFolD, an ed-trace-arrow is checked for a chosen ed-candidate within W, WM, and $WM2$ to adjust the energy and position of the base pair as required. The drawback of this strategy comes from the innate inefficiencies of the trace arrows, meaning an increase in space usage. Recall that within SparseMFEFold, we used strategies such as garbage collection and trace arrow avoidance to save space. These strategies are not, however, possible for SparseRNAFolD-Trace, as an ed-candidate cannot be excluded from the optimal MFE path, and an ed-trace-arrow is therefore required for every ed-candidate.

Bit encoding

Within the second and third strategies, as explained next, we employed bit encoding and bit decoding to store the information about the dangle within the energy values to reduce space usage. Currently, energy values are stored as 32-bits *int* data type. We note that the maximum expected bit usage for the energy value of an RNA sequence of up to 20000 bases is about 13 bits. We employed a bit shift to store the dangle type in the first two bits of the V entries, referred to as V_{enc}, and represented in eq. 8.

$$V_{enc} = (V \ll 2) \mid dangle \tag{8}$$

. Bit decoding technique was used to retrieve the energy value and type/direction of dangle contributions. Bit decoding was done in two steps. Shifting the encoded energy, V_{enc}, two bits forward gave back the energy, V (see eq. 9).

$$V = V_{enc} \gg 2 \tag{9}$$

The dangle type is found in the first two bits; no dangle is represented with a "00" in bits; a 5' dangle with a "01"; a 3' dangle with a "10"; and a 53' dangle with a "11". The dangle type

is decoded using a bit-wise AND with "11" to only keep the first two bits of the encoded energy, as represented in Eq. 10.

$$dangle = V_{enc} \;\&\&\; 11 \tag{10}$$

Strategy 2: Bit encoding with candidate extension

As the second strategy, we used bit encoding within the W and WM entries of the ed-candidate data structure. We refer to this strategy as **SparseRNAFolD-standard**. This implementation of bit encoding was utilized in W and WM entries, as other loop types do not deal with dangles.

Strategy 3: Bit encoding with altered candidate

As the third strategy, we further optimize for space by reducing the candidate size. To reduce candidate size, we stored energy values in ed-candidates in W and WM as V^{d} minus the dangle energy. We refer to this strategy as **SparseRNAFolD-Triplet**. This strategy allows for the correct identification of dangle types regardless of energy parameters used. Note that currently, in the Turner 2004 energy model, the parameter values for 53' dangle for an external loop and multi-loop are the same. These values may be further estimated and revised in future energy models. The extra calculations to retrieve the V^{d} value ensure the accuracy of the result in the event of such a change.

3.3 Compared methods

To evaluate the performance of our SparseRNAFolD, we compared it to two of the best-performing methods for prediction of pseudoknot-free RNA secondary structure, namely RNAFold [9] and LinearFold [8].

3.3.1 RNAFold

RNAFold is part of the Vienna RNA package [9]. As discussed in Section 2.1, RNAfold is an $O(n^3)$ time and $O(n^2)$ space algorithm. It takes an RNA sequence as input and provides the MFE structure as output. RNAFold is well-maintained and highly optimized and is used here as a benchmark for a fast implementation of the Zuker and Steigler-type MFE algorithm.

3.3.2 LinearFold

LinearFold [8] is a pseudoknot-free RNA secondary structure prediction algorithm that uses heuristic techniques to run in linear time and space. As the main goal of sparsification is to speed up the time and space complexity of MFE prediction, we set out to investigate how our SparseRNAFolD compares in practice to LinearFold with better asymptotic complexities.

Linearfold employs two techniques to reduce its time and space complexity to $O(n)$, namely ***beam pruning*** and ***k-best parsing***. Both methods aim to prune the structure path to optimal cases only. Beam pruning works by only keeping a predetermined number (specified by the beam width, b) of the optimal states. Within LinearFold, best sets are kept for each possible loop type as defined in the Zuker algorithm: hairpin, multi-loop fragments, and internal loop. Through beam pruning, time complexity is reduced to $O(nb^2)$ and the space to $O(nb)$ where b is the beam width. K-best parsing further reduces the time to $O(nb\log(b))$. We note that due to the heuristic nature of the LinearFold algorithm, it does not guarantee finding the MFE structure for a given RNA sequence.

4 Experimental Design

We implemented SparseRNAFolD in C++. All experiments were performed using an Azure virtual machine. The virtual machine contained 8 vCPUs with 128 GiB of memory.

4.1 Dataset

We used the original dataset from SparseMFEFold [35]. This dataset is comprised of 3704 sequences in 6 different families selected from the RNAstrand V2.0 database [1]. The smallest sequence is 8 nucleotides long, while the largest is 4381 nucleotides long.

4.2 Energy Model

We used the energy parameters of the Turner 2004 energy model [20, 31], as implemented in the ViennaRNA package [9].

4.3 Accuracy Measures

The number of *true positives* (TP) is defined as the number of correctly predicted base pairings within the structure. The number of *false positives* (FP), similarly, is the number of predicted base pairs that do not exist in the reference structure. Any base missed in the prediction that corresponds to a pairing in the reference structure is a *false negative* (FN).

We evaluate the performance of algorithms based on three measures: sensitivity, positive predictive value (PPV), and their harmonic mean (F-measure).

$$Sensitivity = \frac{TP}{TP + FN} \tag{11}$$

$$PPV = \frac{TP}{TP + FP} \tag{12}$$

$$F_{measure} = \frac{2 \cdot PPV \cdot Sensitivity}{PPV + Sensitivity} \tag{13}$$

4.4 Proof of concept with RNAFold

As a proof of concept for the correct implementation of dangle energy models (i.e., "always dangle" and "exclusive dangle"), we assessed SparseRNAFolD against RNAFold. As the MFE structure may not be unique, we restricted our assessment to the MFE value obtained by each method. We found that the MFE predicted by SparseRNAFolD and RNAFold was the same. Details of the results can be found in our repository.

5 Results

We measured runtime using user time and memory using the maximum resident set size.

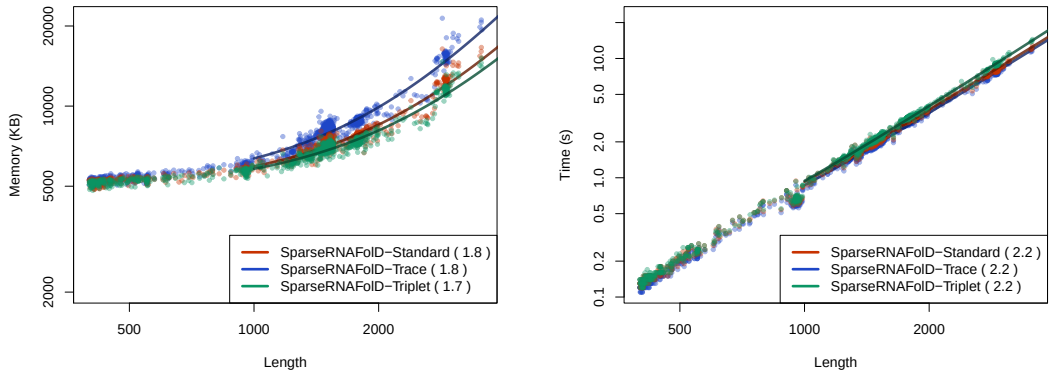

(a) Memory vs Length **(b)** Time vs Length

Figure 2 We plot the results of the three versions of SparseRNAFolD when given RNA sequence only as input against each other and an "exclusive dangle" model based on the dataset. (a) Memory Usage (maximum resident set size in KB) versus length (log-log plot) over all benchmark instances. The solid line shows an asymptotic fit ($c1 + c2n^x$) for sequence length n, constants c1, c2, and exponent x for the fit. We ignored all values < 1000. (b) Run-time (s) versus length (log-log plot) over all benchmark instances. For each tool in both plots, we report (in parenthesis) the exponent x that we estimated from the benchmark results; it describes the observed complexity as $\Theta(n^x)$.

5.1 Alternative Models

We start by comparing the three different implementations of SparseRNAFolD. SparseRNAFolD-standard was found to be in the middle in terms of memory and time. The effect of additional trace arrows in SparseRNAFolD-Trace had a 27% increase in memory usage on the largest sequence compared to SparseRNAFolD-Standard. However, the increase in computation from the bit encoding only resulted in a 5% increase in time on the largest sequence. We find a similar effect when comparing SparseRNAFolD-standard and SparseRNAFolD-Triplet. The altered triplet structure reduced the memory by 9% but increased the time by 10% due to extra computation. These are highlighted in Figure 2.

5.2 Comparison with Linearfold and RNAFold

When comparing SparseRNAFolD-Standard with LinearFold and RNAFold, we look at the "always dangle" model, as LinearFold does not implement the "exclusive dangle" model.

We first compared the three algorithms by their predictive accuracy (F-measure). For comparison, we selected all sequences from our dataset whose structure was available on RNAstrand. We further constrained it to sequences that contained hairpins greater than 3 and no pseudoknots. This resulted in 986 sequences. We found that SparseRNAFolD-Standard had a marginally better, but not significant, average F-measure of 0.6394 compared to 0.6391 of LinearFold. As described in section 4.4, RNAFold and SparseRNAFold-standard are identitcal in predictive accuracy.

We then assessed their time and space usage. To increase the size of our dataset for this testing, we included a dinucleotide shifted version of our dataset in our test data. We then constrained the size of sequences to those > 400. The maximum time and memory used by Linearfold on this dataset were 3.34 seconds and 118,848 KB. The maximum time and memory used by RNAFold were 22.26 seconds and 109136 KB. In contrast, the maximum time and memory spent by SparseMFEFold were 10.86 seconds and 13,000 KB, respectively. This is illustrated in Figures 3b and 3a. The results show that SparseRNAFolD-Standard uses

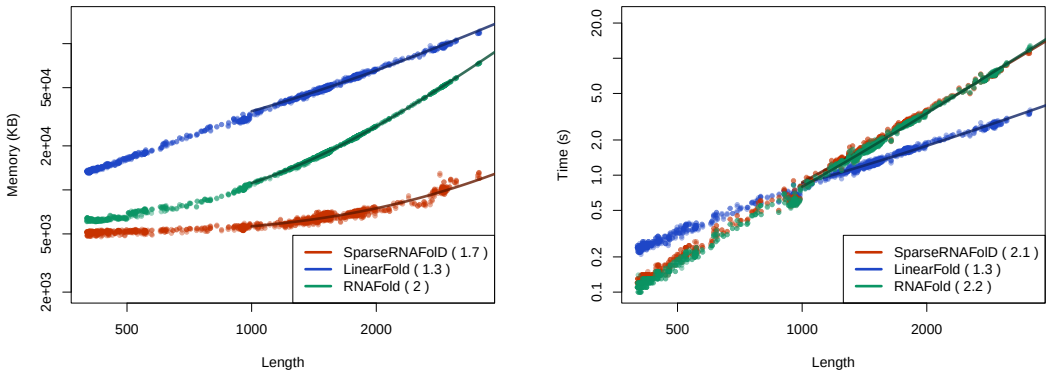

(a) Memory vs Length **(b)** Time vs Length

Figure 3 We plot the results of SparseRNAFolD-Standard against two state of the art algorithms: RNAFold and LinearFold when given RNA sequence only as input against each other and an "always dangle" model on our dataset and the dinucleotide shuffled version of our dataset. (a) Memory Usage (maximum resident set size in KB) versus length (log-log plot) over all benchmark instances. The solid line shows an asymptotic fit ($c1 + c2n^x$) for sequence length n, constants c1,c2, and exponent x for the fit. We ignored all values < 1000. (b) Run-time (s) versus length (log-log plot) over all benchmark instances. For each tool in both plots, we report (in parenthesis) the exponent x that we estimated from the benchmark results; it describes the observed complexity as $\Theta(n^x)$.

	Run-time (s)		Memory: resident set size (KB)	
	RNAfold	SparseRNAFolD	RNAfold	SparseRNAFolD
Minimum	5.04	5.36	40148	8832
Median	7.28	7.86	51284	12592
Maximum	22.08	19.94	109040	16836

Table 1 We tabulate the results of the comparison between RNAFold and SparseRNAFolD-Standard when given only sequences with length > 2500 from our dataset as input and using the "exclusive dangle" model. We looked at time (s) and memory (maximum resident set size in KB) for the minimum, median and maximum length sequence within the constrained dataset.

far less memory on even the largest pseudoknot-free sequences in our dataset. Note that the maximum resident set size is nine times lower than that of LinearFold and eight times lower than that of RNAFold. RNAFold's time remains consistent with SparseRNAFolD-Standard until longer sequences where it fell behind. LinearFold, whose time complexity is $O(nb\log(b))$, where n is the length of the sequence and b is the beam width, did perform faster than SparseRNAFolD-Standard as the length of the sequence increased. However, we did find that SparseRNAFolD-Standard outperformed LinearFold in practice for sequences of up to about 1000 nucleotides.

5.2.1 Highlighting RNAFold

To highlight the difference in space between RNAFold and SparseRNAFolD-Standard, we selected 81 sequences from our dataset with size greater than or equal to 2500. The sequence with the maximum length in the set was 4381 nucleotides long. As seen in Table 1, while SparseRNAFolD-Standard's runtime is comparable to RNAfold's, its memory consumption is about five times lower.

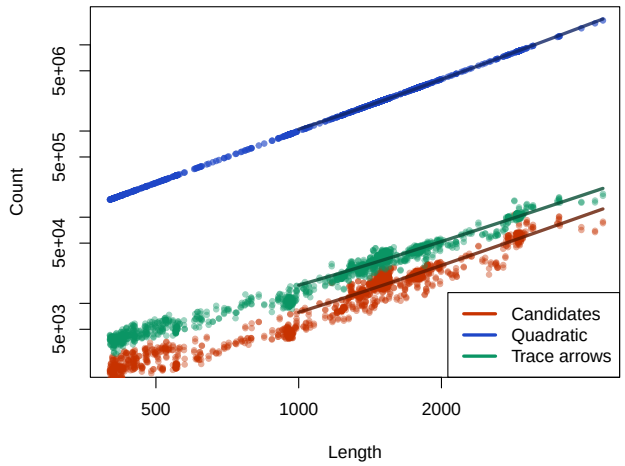

Figure 4 We plot the results of the number of candidates and trace arrows compared to quadratic space. 'Quadratic' shows the count within an nxn matrix as it would be given quadratic space. In contrast, 'Candidates' and 'Trace arrows' show the contrasting number for the same length.

5.3 Candidate Comparison

In order to illustrate the effectiveness of candidates in terms of memory consumption, we plotted the relationship between the number of candidates and trace arrows, against the quadratic space, using the dataset that includes dinucleotide shifted elements. To emphasize the upper limit of candidate usage when executing SparseRNAFolD-Standard, we employ the "exclusive dangle" model.

For a more meaningful comparison, we juxtapose the counts of candidates and trace arrows with the count obtained from a single quadratic matrix. It is important to note that the majority of algorithms employing quadratic space make use of multiple quadratic matrices. Considering this aspect, we discovered that, on average, the disparity in count between the number of candidates and trace arrows with quadratic space was approximately a factor of 100. Figure 4 highlights that the increase in candidates is consistent with the increase in length.

5.4 Folding with Hard Constraints

As partial information on structure has become more available and is extensively used for better prediction of possibly pseudoknotted structures [13, 10], we further extend our evaluation of the SparseRNAFolD versions to cases where we are folding with a hard constraint [17] in addition to the RNA sequence.

To do so, for each sequence, a pseudoknot-free input structure was generated. The structure was generated by taking two random indices at a time from the sequence. If the two bases could pair, were at least 3 bases apart, and did not form a pseudoknot with the other base pairs, the base pair was added to the input structure. In order to avoid overpopulating the input structure, the number of base pairs in an input structure was capped at $0.5 \times \log_2(length)$. This resulted in an average of 3-7 base pairs per sequence. There was a noticeable decrease in time and space when an input structure was provided in addition to an RNA sequence. Between RNA sequence only as input and sequence as well as an input structure, SparseRNAFolD saw a 67% decrease in time and a 40% decrease

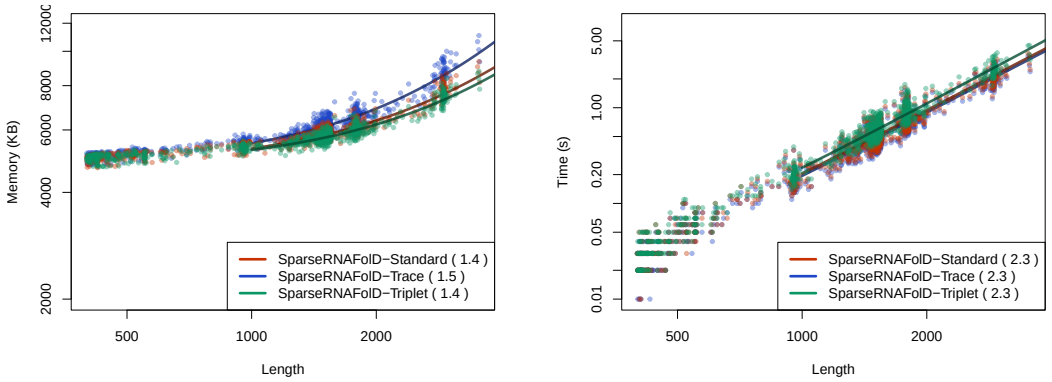

(a) Memory vs Length with a hard constraint

(b) Time vs Length with a hard constraint

Figure 5 We plot the results of the three versions of SparseRNAFolD when given an RNA sequence, an "exclusive dangle" model, and a random pseudoknot-free structure as input against each other based on our dataset. (a) Memory usage (maximum resident set size in KB) versus length (log-log plot) over all benchmark instances. The solid line shows an asymptotic fit ($c1 + c2n^x$) for sequence length n, constants c1,c2, and exponent x for the fit. We ignored all values < 1000. (b) Run-time (s) versus length (log-log plot) over all benchmark instances. For each tool in both plots, we report (in parenthesis) the exponent x that we estimated from the benchmark results; it describes the observed complexity as $\Theta(n^x)$.

in memory. As the input structure reduced the number of candidates for a sequence, the difference in memory was less apparent between the models. SparseRNAFolD-standard had a 6% increase in time from SparseRNAFolD-Trace but a 15% decrease in memory on the largest sequence. From SparseRNAFolD-standard to SparseRNAFolD-Triplet, there was an 8% decrease in memory but a 13% increase in time. Note that even when reducing the number of candidates, the increase in time from Standard to Triplet was greater by 3%. This can be seen in Figure 5.

6 Conclusions

In this work, we introduced SparseRNAFolD, a sparsified MFE RNA secondary prediction algorithm that incorporates dangles contribution to the energy calculation of a sparsified method. We showed that while “no dangle” and “always dangle” models were easy to incorporate into the existing algorithms, “exclusive dangle” introduces non-trivial challenges that need calculated changes to the sparsified recursions to alleviate. We identified three strategies to implement dangle contributions: SparseRNAFolD-Trace which utilizes additional trace arrows; SparseRNAFolD-standard, which incorporates bit encoding as well as extension to the definition of candidate structures; and SparseRNAFolD-Triplet, which, similar to the SparseRNAFolD-standard, utilizes bit encoding but modifies candidate energy calculation in anticipation of possible change in parameters in the future. Comparing these three versions on a large dataset, we concluded that the SparseRNAFolD-Triplet implementation is the most efficient in terms of memory, and SparseRNAFolD-Trace is the most efficient in terms of time. These two versions showcase how space and time trade-offs can improve performance for a specific application. The SparseRNAFolD-standard version provides a middle ground for improvement in both time and space and has been chosen as the standard implementation of our algorithm. While guaranteeing the MFE structure and matching the energy of RNAFold, our SparseRNAFolD is on par with LinearFold on memory usage and

run time for sequences up to about 1000 bases. This provides a promising starting point to bring dangles contributions to pseudoknotted MFE structure prediction methods in which memory usage is the prohibitive factor [14].

Our results showcase the substantial difference in the number of candidates when compared to quadratic space. This provides an illuminating perspective on the space improvement achieved through sparsification.

We further assessed the effect of hard structural constraints on the performance of SparseRNAFolD, presenting significant improvements both in terms of time and space. We believe the significant improvement in time and space due to the limitation of search space by hard structural constraints can have a more pronounced impact on sparsified pseudoknotted MFE prediction, which is our ultimate goal.

Finally, memory consumption becomes a bottleneck for the prediction of MFE structure for long RNA sequences or MFE pseudoknotted structure prediction. Utilizing the power of computational servers, such restrictions have been somewhat alleviated. Sparsification provides improvements in both time and space requirements and can be used to bring computations back to personal computers, providing equal access to the existing technology. In addition, improvements in memory usage can improve use cases for computing clusters, as the amount of memory assigned to a computing node is also limited.

References

1 M Andronescu, V Bereg, H H. Hoos, and A Condon. RNA STRAND: The RNA secondary structure and statistical analysis database. *BMC Bioinformatics*, 9(1):340+, August 2008. doi:10.1186/1471-2105-9-340.

2 R Backofen, D Tsur, S Zakov, and M Ziv-Ukelson. Sparse RNA folding: Time and space efficient algorithms. *Journal of Discrete Algorithms*, 9:12–31, Mar 2011. doi:10.1016/j.jda.2010.09.001.

3 J A. Cruz and E Westhof. The dynamic landscapes of RNA architecture. *Cell*, 136:604–609, Feb 2009. doi:10.1016/j.cell.2009.02.003.

4 S Dimitrieva and P Bucher. Practicality and time complexity of a sparsified RNA folding algorithm. *Journal of Bioinformatics and Computational Biology*, 10, Apr 2012. doi:10.1142/S0219720012410077.

5 R M. Dirks and N A. Pierce. A partition function algorithm for nucleic acid secondary structure including pseudoknots. *Journal of Computational Chemistry*, 24:1664–1677, Aug 2003. doi:10.1017/s1355838298980116.

6 A F. Bompfünewerer et al. Variations on RNA folding and alignment: lessons from Benasque. *Journal of Mathematical Biology*, 56:129–144, Jan 2008. doi:10.1007/s00285-007-0107-5.

7 I L. Hofacker et al. Fast folding and comparison of RNA secondary structures. *Monatshefte für Chemie / Chemical Monthly*, 125:167—188, Feb 1994. doi:10.1007/BF00818163.

8 L Huang et al. Linearfold: linear-time approximate RNA folding by 5'-to-3' dynamic programming and beam search. *Bioinformatics*, 35:i295–i304, Jul 2019. doi:10.1093/bioinformatics/btz375.

9 R Lorenz et al. ViennaRNA package 2.0. *Algorithms for Molecular Biology*, 6, Nov 2011. doi:10.1186/1748-7188-6-26.

10 M Gray, S Chester, and H Jabbari. KnotAli: informed energy minimization through the use of evolutionary information. *BMC Bioinformatics*, 23, May 2022. doi:10.1186/s12859-022-04673-3.

11 I L. Hofacker and P F. Stadler. Memory efficient folding algorithms for circular RNA secondary structures. *Bioinformatics*, 22:1172–1176, May 2006. doi:10.1093/bioinformatics/btl023.

12 C E. Holt and S L. Bullock. Subcellular mRNA localization in animal cells and why it matters. *Science*, 326:1212–1216, Sep 2013. doi:10.1126/science.1176488.

13 H Jabbari and A Condon. A fast and robust iterative algorithm for prediction of RNA pseudoknotted secondary structures. *BMC Bioinformatics*, 15, May 2014. doi:10.1186/1471-2105-15-147.

14 H Jabbari, I Wark, C Montemagno, and S Will. Knotty: efficient and accurate prediction of complex RNA pseudoknot structures. *Bioinformatics*, 34:3849–3856, Nov 2018. doi:10.1093/bioinformatics/bty420.

15 H Jabbari, I Wark, C Mothentemagno, and S Will. Sparsification enables predicting kissing hairpin pseudoknot structures of long RNAs in practice. In *17th International Workshop on Algorithms in Bioinformatics (WABI 2017)*, volume 88 of *Leibniz International Proceedings in Informatics (LIPIcs)*, pages 12:1–12:13. Schloss Dagstuhl–Leibniz-Zentrum fuer Informatik, 2017. doi:10.4230/LIPIcs.WABI.2017.12.

16 M Kozak. Regulation of translation via mRNA structure in prokaryotes and eukaryotes. *Gene*, 361:13–37, Nov 2005. doi:10.1016/j.gene.2005.06.037.

17 R Lorenz, I L. Hofacker, and P F. Stadler. RNA folding with hard and soft constraints. *Algorithms for Molecular Biology*, 11, Apr 2016. doi:10.1186/s13015-016-0070-z.

18 K C. Martin and A Ephrussi. mRNA localization: Gene expression in the spatial dimension. *Cell*, 136:719–730, Feb 2009. doi:10.1016/j.cell.2009.01.044.

19 D H. Mathews and D H. Turner. Prediction of RNA secondary structure by free energy minimization. *Current Opinion in Structural Biology*, 16(3):270–278, Jun 2006. doi:10.1016/j.sbi.2006.05.010.

20 D H. Matthews, M D. Disney, J L. Childs, S J. Schroeder, M Zuker, and D H. Turner. Incorporating chemical modification constraints into a dynamic programming algorithm for prediction of RNA secondary structure. *Proceeding of the National Academy of Science of the USA*, 101:7287–7292, May 2004. doi:10.1073/pnas.0401799101.

21 J S. McCaskill. The equilibrium partition function and base pair binding probabilities for RNA secondary structure. *Biopolymers*, 29:1105–1119, Jun 1990. doi:10.1002/bip.360290621.

22 M Mohl, R Salari, S Will, R Backofen, and S Sahinalp. Sparsification of RNA structure prediction including pseudoknots. *Algorithms for Molecular Biology*, 5, Dec 2010. doi:10.1186/1748-7188-5-39.

23 S A. Mortimer, M A. Kidwell, and J A. Doudna. Insights into RNA structure and function from genome-wide studies. *Nature Reviews Genetics*, 15:469—479, May 2014. doi:10.1038/nrg3681.

24 J Nowakowski and I Tinoco. RNA structure and stability. *Seminars in Virology*, 8(3):153–165, 1997. doi:10.1006/smvy.1997.0118.

25 B Rastegari and A Condon. Parsing nucleic acid pseudoknotted secondary structure: Algorithm and applications. *Journal of Computational Biology*, 14, Mar 2007. doi:10.1089/cmb.2006.0108.

26 J Ren, B Rastegari, A Condon, and H H. Hoos. HotKnots: Heuristic prediction of RNA secondary structures including pseudoknots. *RNA*, 11:1494–1504, Oct 2005. doi:10.1261/rna.7284905.

27 J S. Reuter and D H. Matthews. RNAstructure: software for RNA secondary structure prediction and analysis. *Proceeding of the National Academy of Science of the USA*, 11, Mar 2010. doi:10.1186/1471-2105-11-129.

28 E Rivas and S R. Eddy. A dynamic programming algorithm for RNA structure prediction including pseudoknots. *Journal of Molecular Biology*, 285:2053–2068, Feb 1999. doi:10.1006/jmbi.1998.2436.

29 R Salari, M Möhl, S Will, S Sahinalp, and R Backofen. Time and space efficient RNA-RNA interaction prediction via sparse folding. In *Lecture Notes in Computer Science*, volume 6044, pages 473–490. Research in Computational Molecular Biology, 2010. doi:10.1007/978-3-642-12683-3_31.

30 N Sugimoto, R kierzek, and D H. Turner. Sequence dependence for the energetics of dangling ends and terminal base pairs in ribonucleic acid. *Biochemisty*, 19:4554—-4558, Jul 1987. doi:10.1021/bi00388a058.

31 D H. Turner and D H. Matthews. NNDB: the nearest neighbor parameter database for predicting stability of nucleic acid secondary structure. *Nucleic Acids Research*, 38:D280––D282, Oct 2009. doi:10.1093/nar/gkp892.

32 M B. Warf and J A. Berglund. Role of RNA structure in regulating pre-mRNA splicing. *Trends Biochem Sci.*, 35:169–178, Mar 2010. doi:10.1016/j.tibs.2009.10.004.

33 A Waugh, P Gendron, R Altman, J W. Brown, D Case, D Gautheret, S C. Harvey, N Leontis, J Westbrook, E Westhof, M Zuker, and F Major. RNAML: A standard syntax for exchanging RNA information. *RNA*, 8:707–717, Jun 2002. doi:10.1017/s1355838202028017.

34 Y Wexler, C Zilberstein, and M Ziv-Ukelson. A study of accessible motifs and RNA folding complexity. *Journal of Computational Biology*, 14:856–872, Aug 2007. doi:10.1089/cmb.2007.R020.

35 S Will and H Jabbari. Sparse RNA folding revisited: space-efficient minimum free energy structure prediction. *Algorithms for Molecular Biology*, 11, Apr 2016. doi:10.1186/s13015-016-0071-y.

36 T J. Wilson and D M. J. Lilley. RNA catalysis—is that it? *RNA*, 21:534–537, Apr 2015. doi:10.1261/rna.049874.115.

37 J Zuber, B J. Cabral, I McFayden, D M. Mauger, and D H. Matthews. Analysis of RNA nearest neighbor parameters reveals interdependencies and quantifies the uncertainty in RNA secondary structure prediction. *RNA*, 24:1568–1582, Nov 2018. doi:10.1261/rna.065102.117.

38 J Zuber, H Sun, X Zhang, I McFayden, and D H. Matthews. A sensitivity analysis of RNA folding nearest neighbor parameters identifies a subset of free energy parameters with the greatest impact on RNA secondary structure prediction. *Nucleic Acids Research*, 45:6168—-6176, Jun 2017. doi:10.1093/nar/gkx170.

39 M Zuker. Mfold web server for nucleic acid folding and hybridization prediction. *Nucleic Acids Research*, 31:3406–3415, Jul 2003. doi:10.1093/nar/gkg595.

40 M Zuker and A B. Jacobson. Using reliability information to annotate RNA secondary structures. *RNA*, 4:669–679, Jun 1998. doi:10.1017/s1355838298980116.

41 M Zuker and P Stiegler. Optimal computer folding of large RNA sequences using thermodynamic and auxiliary information. *Nucleic Acids Research*, 9:133–148, Jan 1981. doi:10.1093/nar/9.1.133.

42 M Zuker and P Stiegler. Optimal computer folding of large RNA sequences using thermodynamics and auxiliary information. *Nucleic Acids Research*, 9:133–148, Jan 1981. doi:10.1093/nar/9.1.133.

7 Author contributions statement

MG and HJ conceived the experiment(s), MG. conducted the experiment(s), M.G. analysed the results. M.G. and H.J. and S.W. wrote and reviewed the manuscript.